Eur Biophys J (2003) 32: 1–11
DOI 10.1007/s00249-002-0260-0

ARTICLE

Koka Yonebayashi · Satoru Yamaguchi · Satoru Tuzi
Hazime Saitô

Cytoplasmic surface structures of bacteriorhodopsin modified by site-directed mutations and cation binding as revealed by ^{13}C NMR

Received: 13 June 2002 / Revised: 30 September 2002 / Accepted: 3 October 2002 / Published online: 1 November 2002

Abstract We have examined how cytoplasmic surface structures of [3-^{13}C]Ala-labeled bacteriorhodopsin (bR), consisting of the C-terminal α-helix and cytoplasmic loops, are altered by site-directed mutations at the former (R227Q) and the latter (A160G, E166G, and A168G) and by cation binding, by means of displacements of the ^{13}C NMR peaks of Ala228 and Ala233 (C-terminal α-helix), Ala103 (C-D loop), and Ala160 (E-F loop). Cytoplasmic ends of the B and F helices were found to undergo fluctuation motions on the order of 10^{-5} s, when such surface structures were disrupted, as viewed from suppressed ^{13}C NMR signals. This happens also for deionized blue membranes of wild type and A160G, with accelerated fluctuations in the loops. Further, cytoplasmic surface structures of Na^+-regenerated purple membrane from the blue membrane were significantly modified by Ca^{2+} ions up to 1 mM under relatively low ionic strength of 10 mM NaCl, although they are very similar at high ionic strength (100 mM NaCl). To interpret these findings, the following two surface structures were proposed. The C-terminal α-helix of the wild type at ambient temperature is involved in a perturbed type, probably tilted toward the direction of the B and F helices, to prevent unnecessary fluctuations of these helices for efficient proton uptake during the photocycle. An unperturbed type of helix is achieved when such a surface structure was disrupted at low temperature or in an M-like state. This view is consistent with previously published data for the ''proton binding cluster'' consisting of Asp104, Glu166, and Glu234.

Keywords Surface dynamics · Bacteriorhodopsin · Carbon-13 NMR · Site-directed mutation · Cation binding

K. Yonebayashi · S. Yamaguchi · S. Tuzi · H. Saitô (✉)
Department of Life Science,
Graduate School of Science,
Himeji Institute of Technology,
Harima Science Garden City, Kouto 3-chome,
Kamigori, Hyogo 678-1297, Japan
E-mail: saito@sci.himeji-tech.ac.jp

Abbreviations *bR*: bacteriorhodopsin · *CP-MAS*: cross polarization-magic angle spinning · *DD-MAS*: dipolar decoupled-magic angle spinning

Introduction

Bacteriorhodopsin (bR) is a light-driven proton pump in the purple membrane of *Halobacterium salinarum* and is considered to be a prototype of biologically important membrane proteins consisting of a bundle of seven transmembrane α-helices and interhelical loops. The three-dimensional structures of bR in two- and three-dimensional crystals have been determined by cryo-electron microscopy and X-ray diffraction, respectively (Henderson et al. 1990; Grigorieff et al. 1996; Kimura et al. 1997; Pebay-Peyroula et al. 1997; Essen et al. 1998; Luecke et al. 1998, 1999; Mitsuoka et al. 1999; Sato et al. 1999). The revealed structures of the transmembrane α-helices are generally consistent, but their surface structures are either obscured or inconsistent with each other. One reason for this inconsistency in the surface structures may be that they are not always static as anticipated from such diffraction studies, even at low temperature, but are undergoing motional fluctuations with a range of motional frequencies. As a result, their averaged structures could be largely modified by a variety of intrinsic or environmental factors such as ionic strength, temperature, pH, site-directed mutations (Saitô et al. 2000; Yamaguchi et al. 2001a), or crystallographic contacts (Heymann et al. 1999; Müller et al. 2000). Thus, it is not easy to obtain structural data of intact surface structures which are relevant to physiological conditions by diffraction studies alone, because such dynamic or structural disorder is overwhelming at ambient temperature.

In contrast, we have demonstrated that the ^{13}C NMR approach is an excellent, non-perturbing alternative means to clarify dynamic as well as conformational aspects of membrane proteins, utilizing the conformation-dependent displacement of ^{13}C NMR

peaks, as an intrinsic probe, so far accumulated for any given peptide units (Saitô 1986; Saitô and Ando 1989; Saitô et al. 1998, 2002), if the ^{13}C NMR signals of interest are well separated from different sites and subsequently assigned to such particular amino acid residues. In practice, it turned out that up to twelve ^{13}C NMR peaks were resolved for [3-^{13}C]Ala- or [1-^{13}C]Val-labeled bR of fully hydrated samples, depending upon their locations for any given labeled amino-acid residues with specific local conformations among 29 Ala or 21 Val residues, respectively (Tanio et al. 1999; Tuzi et al. 1999; Yamaguchi et al. 2000, 2001a). The major advantage of this ^{13}C NMR approach is that dynamic features of particular sites, such as C-terminal residues, including the C-terminal α-helix portion protruding from the membrane surface and loops, and transmembrane α-helices are readily distinguishable on the basis of their ^{13}C spin-lattice relaxation times, selectively suppressed ^{13}C NMR signals due to the failure of attempted peak-narrowing by the presence of interference with either proton decoupling or magic angle spinning. As demonstrated, however, these C-terminal α-helix and loops are not present independently but assembled to form a unique surface structure, depending upon a variety of environmental factors, such as pH, temperature, ionic strength, etc. (Yamaguchi et al. 2001a).

Cation binding can be considered as a possible perturbant to such surface structures, because there are several negatively charged residues in the cytoplasmic surface (see the marked residues by the ovals in the schematic representation of the primary and secondary structure of bR in Fig. 1). The presence of the specific cation-binding site was initially proposed in relation to the alteration of the color and function of bR (Chang et al. 1985; Ariki and Lanyi 1986). In contrast, Szundi and Stoeckenius (1987, 1989) showed that lowered surface pH, induced by the removal of surface bound cations, can explain the purple to blue transition. This view is consistent with the similarity of the ^{13}C NMR spectra of [3-^{13}C]Ala-labeled bR between the cation-free and acid-blue membranes. The most preferred binding site for divalent cations is at the extracellular side near Ala196 instead of the expected site near Asp85 (Tuzi et al. 1999). Recently, Váró et al. (1999) suggested that cation binding occurs nonspecifically at the membrane

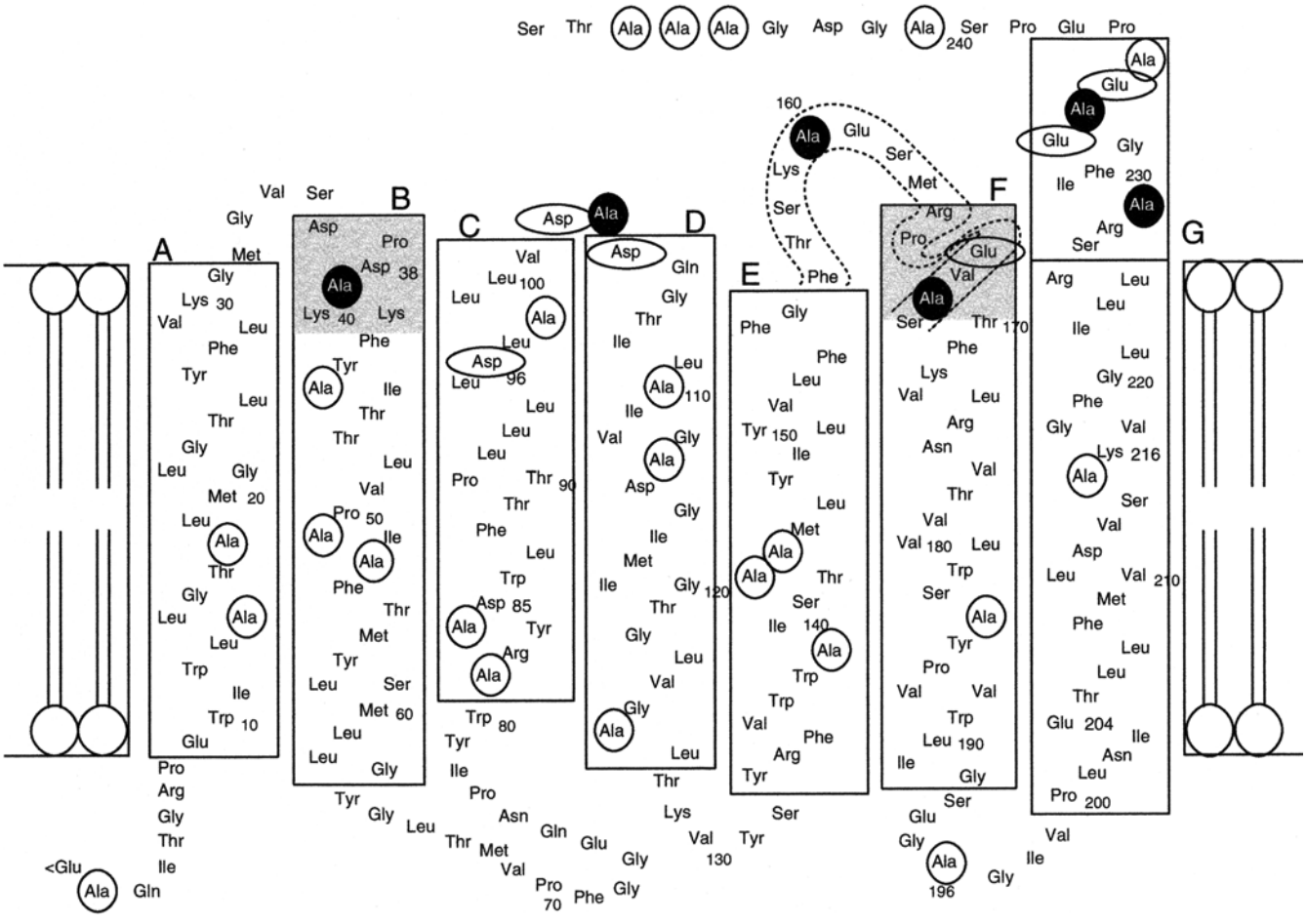

Fig. 1 Schematic representation of the secondary structure of bR based on X-ray diffraction (Luecke et al. 1998). All Ala residues labeled by [3-^{13}C]alanine are indicated by *circles*, while the transmembrane α-helices (A-G) and C-terminal α-helix (G′), as identified by X-ray diffraction and previous ^{13}C NMR studies, respectively, are indicated by *rectangular boxes*. In particular, Ala and acidic residues in the cytoplasmic surface are colored *black* and indicated by *ovals*, respectively, and residues at the vicinity of the E-F loops are indicated by a *dotted strip*

surface and influences the protonation state of Asp85 through the surface pH, although some experimental data favor a view of a specific cation-binding site (Jonas and Ebrey 1991; Zhang and El-Sayed 1993; Tan et al. 1996; Pardo et al. 1998). We have so far proposed the presence of a cytoplasmic surface complex consisting of the C-terminal α-helix and interhelical C-D and E-F loops through formation of salt bridges between charged residues or metal ion-mediated interactions. The stability of the complex varies with a variety of environmental factors as mentioned above, as manifested by the ^{13}C NMR feature of the C-terminal α-helix and loops (Tuzi et al. 1994; Saitô et al. 2000; Yamaguchi et al. 2001a). In this connection, it is interesting to note that the ^{13}C NMR spectrum of Na^+-regenerated [3-^{13}C]Ala-labeled purple membrane by the addition of Na^+ ions without divalent cations turned out to be not always the same as that of the native purple membrane (Tuzi et al. 1999). This finding strongly suggests a possibility that the cytoplasmic surface structure could be modified with and without divalent cations bound to various types of cytoplasmic cation-binding sites, in addition to the more preferred site at the extracellular side (Tuzi et al. 1999). This view is consistent with a recent finding together with a possible site for the negatively charged lipid molecules (Eliash et al. 2001; Wang and El-Sayed 2001).

Further, several pieces of evidence have been presented on how specific surface electrical charges at the cytoplasmic surface are involved in efficient proton uptake during the photocycle in relation to the biological significance of the above-mentioned surface complex. Riesle et al. (1996) proposed that the surface-exposed amino acids Asp36 (A-B loop), Asp102 and Asp104 (C-D loop), and Glu161 (E-F loop) seem to efficiently collect protons from the aqueous bulk phase and funnel them to the entrance of the cytoplasmic proton pathway. Checover et al. (1997, 2001) showed that a dominant "proton binding cluster" of the wild-type protein consists of Asp104, Glu161, and Glu234 (C-terminal α-helix), together with Asp36 as a mediator to deliver the proton to a channel. In particular, replacement of Glu234 (C-terminal α-helix, designated by G′ in Fig. 1) with cysteine disrupted the structure of the cluster (Checover et al. 2001), probably through disruption of the surface structure. Naturally, it is anticipated that the presence of such a cluster is strongly related to the above-mentioned cytoplasmic surface structure which could be readily modified by surface charge through formation of salt bridges and/or bound metal ions.

More directly, however, it is anticipated that such a surface structure could be altered by site-directed mutations at the key positions mentioned above, through modified salt bridges and/or metal ion-mediated interactions. Here, we aimed to clarify how such surface structures could be varied by site-directed mutations at the C-terminal α-helix (R227Q) and in the vicinity of the E-F loop (A168G, E166G, and A160G) (drawn by dotted strip in Fig. 1), which are important for formation of the so-called "proton binding cluster" (Checover et al. 2001). We further performed comparative studies on the wild type and A160G as to how their surface structures are altered by deionization, regenerated purple membranes with or without divalent cations, and temperature, in relation to understanding their biological significance.

Materials and methods

Sample preparation

[3-^{13}C]-L-Ala was purchased from CIL (Andover, Mass., USA) and used without purification. *Halobacterium salinarum* S9 and R227Q, E166G, A168G, and A160G mutants were grown in temporary synthetic medium (Onishi et al. 1965) in which unlabeled L-Ala was replaced by [3-^{13}C]-L-Ala in the circled positions in Fig. 1. Purple membrane-containing bR was isolated by the method of Oesterhelt and Stoekenius (1974) and suspended in 5 mM HEPES buffer at pH 7 containing 0.02% NaN_3 and 10 mM NaCl. Deionized blue membranes were prepared by suspending purple membrane (15 mg) in distilled water contained in plastic vessels and incubated with cation exchange resin Dowex 50W-X8 (bed volume 20 mL) until the absorption maximum of the chromophore shifted from 568 nm to 603 nm (at 40 °C for 1–2 h). The deionized membrane was washed twice with high-purity water (resistivity 18 MΩ cm) and then resuspended in the same. Na^+-regenerated purple membrane (∼15 mg) was prepared by adjustment of the bulk pH of the deionized membrane to pH 7 by titration with 0.01 M NaOH (Tuzi et al. 1999) and precipitated twice by centrifuge (Na^+ purple membrane in Na^+ buffer). For the preparation of the Na^+/Ca^{2+}-regenerated purple membrane, the following three kinds of buffer solutions containing 1 M, 100 mM, and 5 mM $CaCl_2$ were prepared. To Na^+-regenerated bR (∼15 mg) suspended in the Na^+ buffer (by adjusting the absorption of 568 nm to 1.000), 1/1000 volume of the above-mentioned Ca^{2+} buffer solutions was added, followed by precipitation by centrifuge. The bR:Ca^{2+} ratios were 1:62.9, 1:6.29, and 1:0.314, when the first, second, and third Ca^{2+} buffer solutions, respectively, were utilized. In a similar manner, Na^+/Mn^{2+}-regenerated purple membrane of the A160G mutant was prepared to remove ^{13}C NMR signals from the surface areas due to accelerated spin-spin relaxation by the paramagnetic Mn^{2+} ion (Tuzi et al. 2001).

Samples for ^{13}C NMR spectra (∼10 mg) were concentrated by centrifugation and placed into a 5 mm outer diameter zirconia pencil-type rotor for magic angle spinning. Sample rotors were tightly sealed by Teflon caps and the caps were glued to the rotor by rapid Alardyte to prevent dehydration of pelleted samples through any pin-hole in the caps during magic angle spinning under a stream of dried compressed air.

NMR measurements

^{13}C NMR spectra were recorded at 100.64 MHz at ambient temperature (20 °C) in the dark on a Chemagnetics CMX-400 NMR spectrometer by dipolar decoupled-magic angle spinning (DD-MAS) and cross polarization-magic angle spinning (CP-MAS) methods, which allow detection of [3-^{13}C]Ala-labeled ^{13}C signals from the whole area and less mobile regions such as the transmembrane α-helices and loops, respectively. The spectral width, contact, repetition, and acquisition times for the latter were 40 kHz, 1 ms, 4 s, and 50 ms, respectively. Free induction decays were acquired by 2k data points and accumulated more than 5000 times until a reasonable signal-to-noise ratio was achieved. Fourier transform was carried out as 16k points after 14k points were zero-filled. ^{13}C chemical shifts were referred to the carboxyl signals of glycine (176.03 ppm) and then converted to values with reference to tetramethylsilane (TMS).

Results

Figure 2 compares the ^{13}C CP-MAS (left) and DD-MAS (right) NMR spectra of [3-^{13}C]Ala-labeled E166G (A), A168G (B), and R227Q (C) with those of wild type (D), in order to assign the ^{13}C C_β peak position of Ala168 (B) and to delineate a conformational change of the cytoplasmic surface complex between the C-terminal α-helix, A-B, C-D, and E-F loops caused by site-directed mutation at the C-terminal α-helix (R227Q) and in the vicinity of the E-F loop [E166G (A) and A168 (B)]. Interestingly, the resultant spectral changes among the three mutants are very similar. In particular, several peaks marked by the arrows were suppressed or displaced in the ^{13}C NMR spectra of the mutants with reference to those of the wild type (WT) (Fig. 2D). Notably, the spectral change in the loop region is that the two peaks with equal intensity at 17.19 and

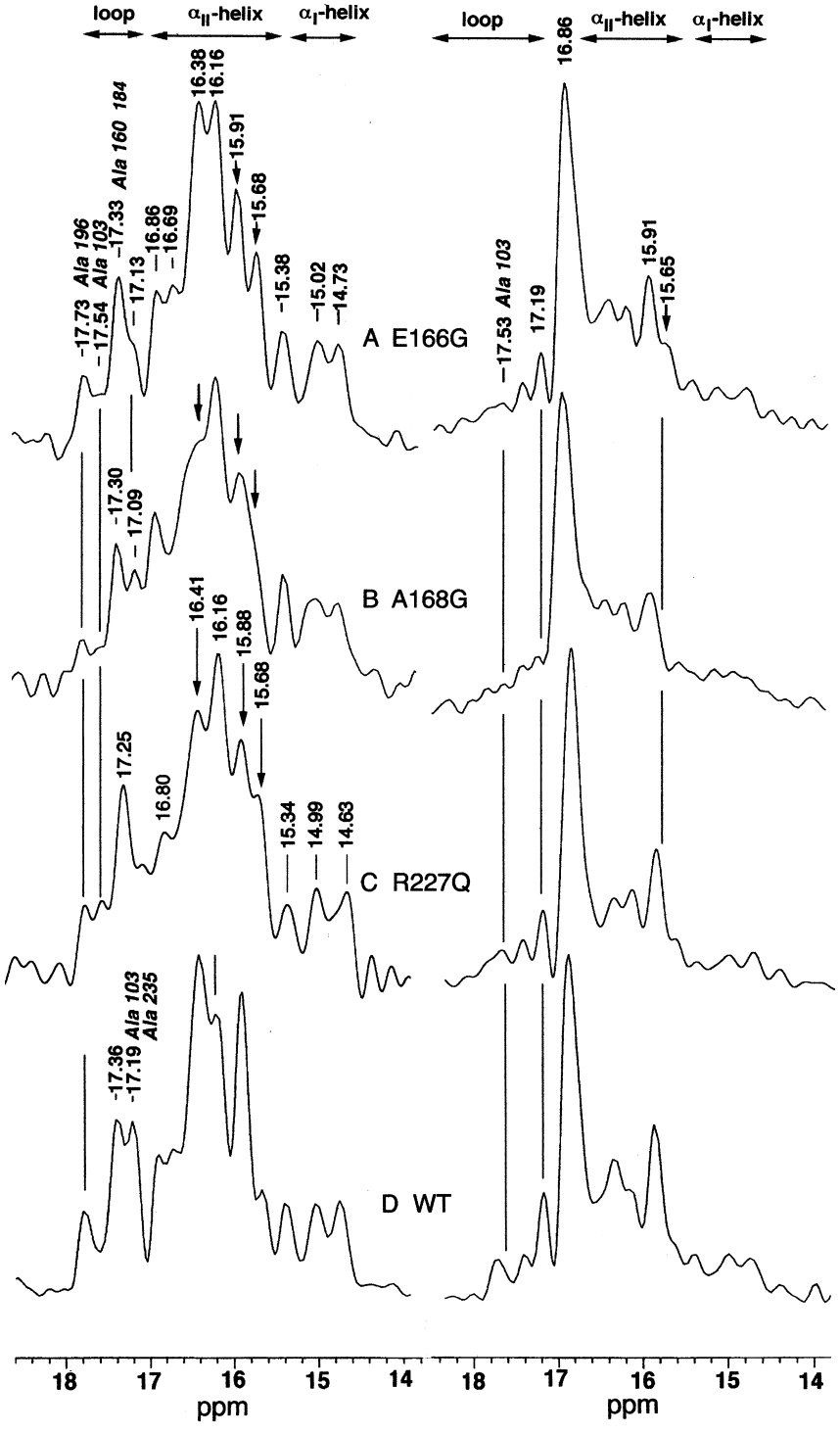

Fig. 2 ^{13}CP-MAS (*left*) and DD-MAS (*right*) NMR spectra of [3-^{13}C]Ala-labeled E166G (**A**), A168G (**B**), and R227Q (**C**) as compared with those of the wild type recorded at pH 7, 20 °C, and 10 mM NaCl solution (**D**)

17.36 ppm of the WT changed to an asymmetric pattern in these mutants, mainly due to the downfield displacement of the upper field peak of the doublet from 17.19 ppm of Ala103 (under 10 mM NaCl, Fig. 2D) to 17.54 ppm in these mutants (Yamaguchi et al. 2000, 2001a). The latter peak emerges as a shoulder peak of an elevated ravine in the CP-MAS spectra (A and B), but is more clearly distinguished as a resolved peak in the corresponding peak position for the R227Q mutant in Fig. 2C. This peak position is also visible in the DD-MAS NMR spectra (marked by the vertical line in the spectra on the right-hand side) at the expense of decreased peak intensity at 17.19 ppm. The C_β Ala168 peak was straightforwardly ascribed to 16.38 ppm, which was most significantly reduced for A168G as compared with that of the WT, although this peak is superimposed upon the Ala39 peak previously assigned (Yamaguchi et al. 2000). It is notable that the Ala39 peak at 16.38 ppm is displaced upfield to 16.16 ppm for the R227Q mutant owing to an accompanied conformational change for this mutation. Besides, the intense 15.91 ppm peak from the C-terminal α-helix of the WT appears to split into the two arrowed peaks for E166G, A168G, and R227Q mutants; one of the peaks is displaced up field to 15.68 ppm (Fig. 2A–C).

It turned out that the ^{13}C NMR spectra of regenerated bR prepared by addition of Na^+ of low ionic strength (10 mM) (without divalent cations) are not always the same as those of the intact preparation (Fig. 3A), although both preparations exhibit the same purple color. In particular, the intensities of the three ^{13}C CP-MAS NMR peaks (Fig. 3A, left), at 17.20 (Ala103 and Ala235), 16.89 (Ala84), and 15. 91 ppm (Ala228 and Ala233 of the C-terminal α-helix), of the intact preparation (dotted trace) were significantly reduced for the regenerated preparation (solid trace). The downfield displacement of the Ala103 peak from 17.20 ppm to 17.53 ppm is consistent with the observations of the site-directed mutants (Fig. 2). This type of spectral change is more evident when 5 μM Ca^{2+} ion is added to this preparation (in the presence of 10 mM Na^+ ion; Na^+/Ca^{2+}-regenerated purple form) (Tuzi et al. 1999). In contrast, further addition of the Ca^{2+} ion up to 1 mM caused an upfield displacement of the intense peak (Ala160) from 17.36 to 17.20 ppm (Fig. 3B–D, Table 1). The CP-MAS peak intensity at 15.91 ppm remains reduced during this procedure, although this peak is fully visible by DD-MAS NMR.

The Na^+-regenerated WT bR from the blue membrane was obtained by addition of 100 mM Na^+, as shown in Fig. 4 (gray line). Interestingly, this spectrum gives rise to almost the same ^{13}C NMR pattern as the intact preparation of bR (solid line), although the intact preparation yielded better spectral resolution, in contrast to the case of the A160G mutant in which more pronounced spectral resolution is achieved for the regenerated preparation, as will be discussed later (see Fig. 6).

Figure 5 illustrates the very similar spectral patterns of the ^{13}C CP-MAS (left) and DD-MAS (right) NMR

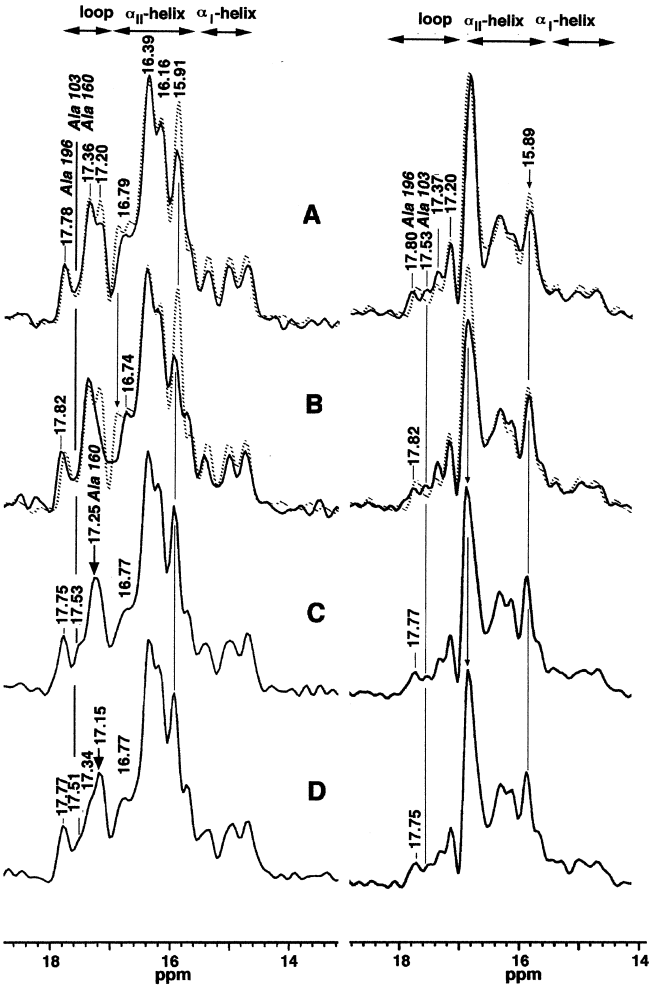

Fig. 3 ^{13}CP-MAS (*left*) and DD-MAS (*right*) NMR spectra of [3-^{13}C]Ala-labeled Na^+-regenerated purple membrane (10 mM Na^+) (**A**), Na^+/Ca^{2+}-regenerated in the presence of 5 μM Ca^{2+} and 10 mM Na^+ (**B**), 100 μM Ca^{2+} and 10 mM Na^+ (**C**), and 1 mM Ca^{2+} and 10 mM Na^+ (**D**). ^{13}C CP-MAS and DD-MAS spectra of the WT at 10 mM NaCl are indicated as *dotted traces*

spectra of the deionized [3-^{13}C]Ala-labeled WT (top) and A160G mutant (bottom) of bR, although they differ substantially at neutral pH (dotted lines) (Yamaguchi et al. 2001a). This is apparently caused by several kinds of spectral changes: suppressed signals at the loop region, 17.75 ppm (Ala196 at the F-G loop), 17.36 ppm (Ala160, E-F loop), and 17.20 ppm (Ala103, C-D loop) (in the presence of 10 mM NaCl); upfield displacement of a peak at 17.27 ppm, ascribable to Ala184 in the transmembrane α-helix F or Ala235 of the C-terminal α-helix or both from the superimposed peak upon the regions of 17.36 and 17.20 ppm, to the peak position of 17.00 ppm; equally suppressed peak at 16.38 ppm of the WT type ascribable to Ala39 and Ala168; and recovery of the peak at 15.74 ppm arising from Ala228 and Ala233 of the C-terminal α-helix for the A160G mutant. Most notably, the peak positions of the C-terminal α-helix of the blue membrane, 15.76 and 15.74 ppm for

Table 1 Displacements of ^{13}C chemical shifts of the C-terminal α-helix and loops from [3-^{13}C]Ala-labeled bacteriorhodopsin and its mutants

		C-terminal α-helix: Ala228, Ala233 (ppm)	Loop (ppm)		Ref
			Ala103	Ala160	
Wild type	20 °C[a]	15.91	17.19	17.36	b, c
	40 °C	16.40	17.62	–	b, c
	–10 °C	15.50	17.58	17.30	b, c
A160G	20 °C	15.91	17.61	–	This work
	0 °C	15.67	17.43	–	This work
WT	High ionic strength (100 mM NaCl)	15.89	17.56	17.37	b
	Decreased pH (pH 4.5)	15.89/15.67	17.57	17.27	d
	(pH 1.2)	15.76	e	e	d
	Deionized	15.76	e	e	d
	Added Ca^{2+}	15.91	17.51	17.37–17.15	This work
	Papain-cleaved	None	17.52	17.27	b
R227Q	(C-terminal α-helix)	15.88/15.68	17.54	17.28	This work
A228G	(C-terminal α-helix)	15.87	17.58	17.32	b
D85N	(pH 7) (C-helix)	15.84	17.59	17.40	f
	(pH 10) (C-helix)	15.87/15.61	e	e	f
E166G	(F-helix)	15.91/15.68	17.53	17.30	This work
A168G	(F-helix)	15.91/15.68	17.53	17.30	This work

[a]Reference state: pH 7, 10 mM NaCl, 20 °C, unless otherwise specified
[b]Yamaguchi et al. (2001a)
[c]Yamaguchi et al. (2000)
[d]Tuzi et al. (1999)
[e]Peaks suppressed
[f]Kawase et al. (2000)

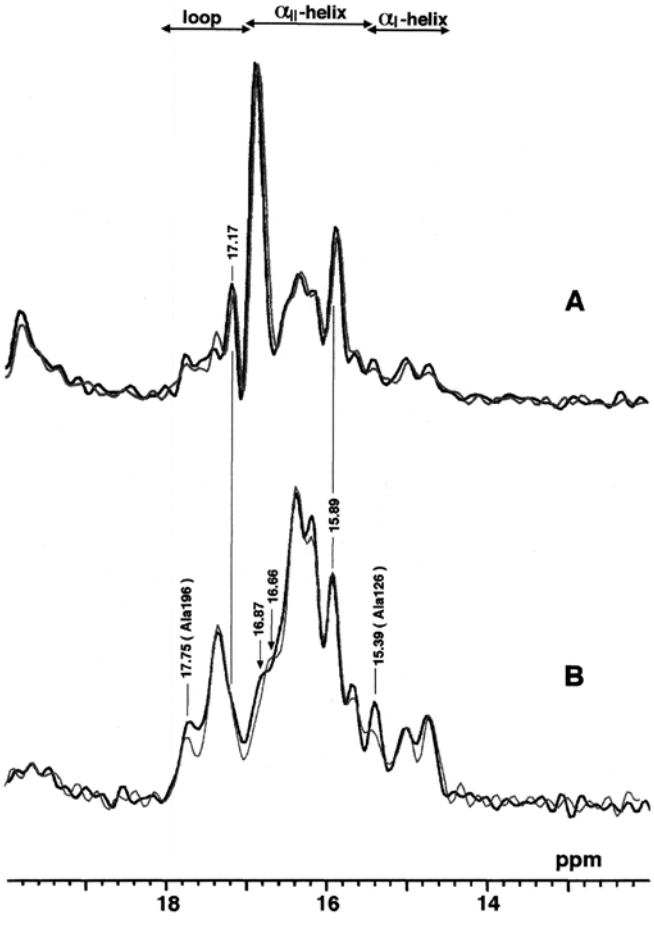

Fig. 4 ^{13}C DD-MAS (**A**) and CP-MAS (**B**) of [3-^{13}C]Ala-labeled intact (*black lines*) and Na^+-regenerated (*gray lines*) bR of the WT in the presence of 100 mM Na^+

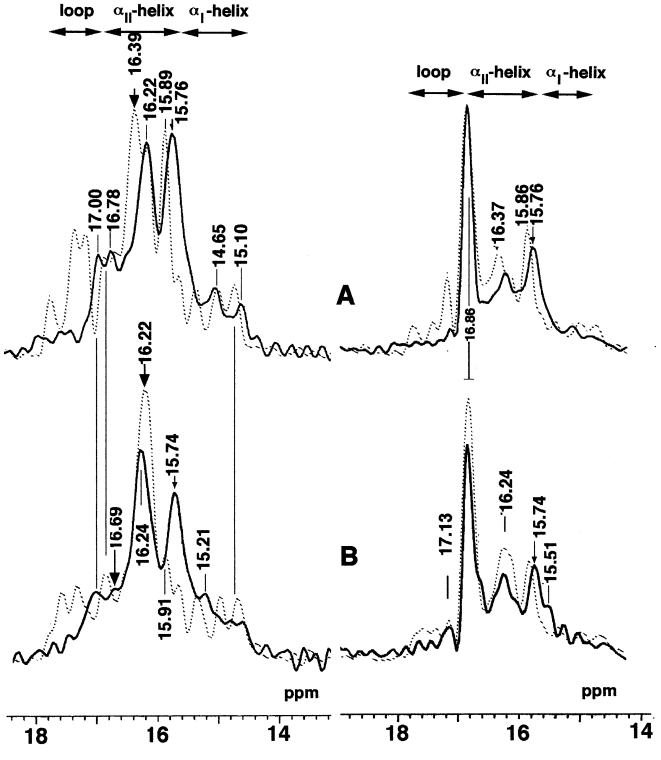

Fig. 5 ^{13}CP-MAS (*left*) and DD-MAS (*right*) NMR spectra of deionized [3-^{13}C]Ala-labeled WT (**A**) and A160G (**B**) of blue membranes as compared with those recorded at neutral pH (purple membrane) (*dotted spectra*)

the WT and A160G, resonate at higher field positions than those of purple membrane by 0.15 and 0.17 ppm, respectively (dotted traces).

Figure 6 compares the ^{13}C CP-MAS NMR spectra of [3-^{13}C]Ala-labeled Na^+/Mn^{2+}-regenerated A160G mutant (in the presence of 50 μM Mn^{2+} and 10 mM Na^+) (A), intact (B), and Na^+-regenerated preparations (10 mM Na^+ only) (C). It is noteworthy that the four well-resolved ^{13}C NMR peaks were clearly visible from the loop region of the regenerated preparation (Fig. 6C)

as compared with those for the intact preparation (Fig. 6B). In the latter, the ^{13}C NMR signals of Ala196 and Ala235 were substantially broadened (Fig. 6B) as compared with those of the regenerated A160G (Fig. 6C). The Ala184 peak (helix F) of the A160G mutant is also superimposed upon the Ala160 signal of the loop region owing to the presence of the kinked structure at Pro186 as encountered for the WT (Tuzi et al. 1999, 2001). This view can be now straightforwardly confirmed by the fact that this peak remains intact as a single peak at 17.33 ppm from residues buried within the inner part of the transmembrane α-helix F, in spite of the presence of the surface-bound Mn^{2+} ion. In fact, ^{13}C NMR signals of several Ala residues located at the surface were suppressed by an accelerated spin relaxation process by Mn^{2+} ions bound to residues in the surface (Fig. 6A) (Tuzi et al. 2001). The peak intensity of the α-helical peak at 16.33 ppm ascribable to Ala39 and Ala168 (Fig. 6A) in the Na^+-regenerated preparation is reduced in the intact preparation (Fig. 6B). Further, it is interesting to note that the ^{13}C NMR peaks of Ala228 and Ala233 from the C-terminal α-helix of the regenerated A160G preparation are displaced upfield when the temperature is lowered from 40 °C (A) to 0 °C (C) (Table 1), whereas the Ala235 peak from the residue at the corner of the C-terminal α-helix (17.18 ppm at 20 °C) is concomitantly displaced downfield to 17.34 ppm at 0 °C, as illustrated in Fig. 7.

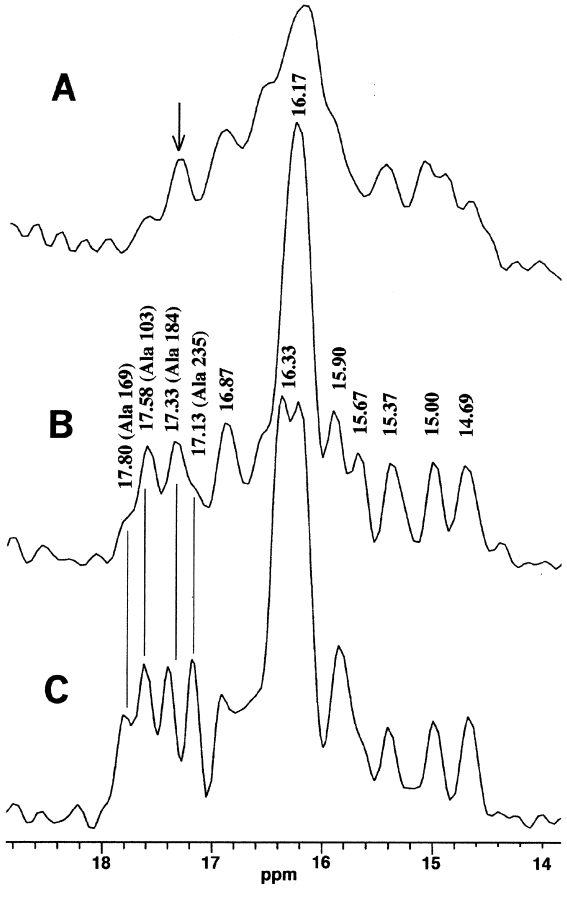

Fig. 6 Comparison of ^{13}C CP-MAS NMR spectra of [3-^{13}C]Ala-labeled, Na^+/Mn^{2+}-regenerated (50 μM Mn^{2+} and 10 mM Na^+) (**A**), intact (**B**), and Na^+-regenerated A160G in the presence of 10 mM Na^+ (**C**)

Discussion

Confirmed assignment of [3-^{13}C]Ala-labeled ^{13}C NMR peaks from the cytoplasmic loops

So far, we have assigned the three well-resolved ^{13}C NMR signals of [3-^{13}C]Ala-labeled bR resonating in the low-field region (17.80–17.20 ppm) in the presence of 10 mM NaCl to Ala196, Ala160, and Ala103 in the loop

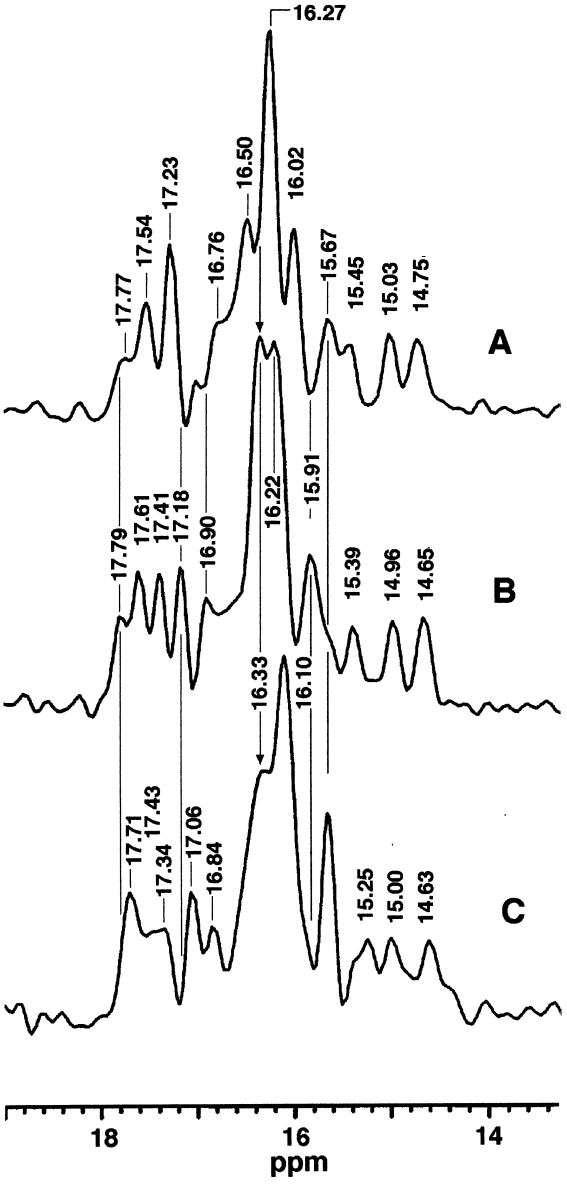

Fig. 7 ^{13}C CP-MAS NMR spectra of [3-^{13}C]Ala-labeled, Na^+-regenerated A160G (10 mM Na^+) at 40 °C (**A**), 20 °C (**B**), and 0 °C (**C**)

region from the low to the high field, respectively (Yamaguchi et al. 2001a, 2001b), although the ^{13}C NMR signals of Ala184 located at the kinked F helix (Tuzi et al. 2001) and Ala235 prior to Pro from the C-terminal α-helix (Tuzi et al. 1999) are also superimposed upon the peak positions at 17.37 and 17.20 ppm, respectively. Nevertheless, the ^{13}C C_β NMR peak of Ala103 was displaced downfield to the peak position of 17.54 ppm by 0.35 ppm by the site-directed mutation [A168G and E166G at the cytoplasmic end of the F helix, and R227Q and A228G at the C-terminal α-helix, as shown in Fig. 2 (Yamaguchi et al. 2001a)]. This peak was also displaced by changing the environmental parameters such as regenerated bR containing 10 mM Na^+ alone (Fig. 3), increased ionic strength to 100 mM NaCl (Fig. 4), lowered pH to 4.5, or raised temperature to 40 °C (Yamaguchi et al. 2001a). The assignment of the Ala184 peak was further confirmed as a remaining peak at 17.33 ppm in the ^{13}C NMR spectrum of Mn^{2+}-treated A160G mutant in which most of the ^{13}C NMR signals from Ala residues located near the membrane surfaces were suppressed (arrowed peak, Fig. 6A). It is emphasized that the ^{13}C C_β peak position of Ala103 also resonates at 17.58 ppm for the A160G mutant under the regenerated conditions at 10 mM Na^+ (Fig. 6C). In contrast, the Ala160 signal of the WT is found to be displaced upfield, from 17.36 to 17.15 ppm, by adding Ca^{2+} ion up to 1 mM in the presence of 10 mM Na^+ ion (Fig. 3). Undoubtedly, such mutual displacements of the peaks from Ala103 and Ala160 arise from the resulting conformational changes in these loop regions induced mainly by the above-mentioned changes in the environmental factors or site-directed mutation both at the E-F loop and C-terminal α-helix. The most obvious consequence of these findings is that they are held together to lead to the surface structure or cytoplasmic complex at the cytoplasmic surface through formation of salt bridges between charged residues and/or metal binding. It is emphasized that the identification of either displaced or suppressed peaks at several Ala residues, located at the key positions in the cytoplasmic surface marked in black in Fig. 1, can be conveniently utilized as intrinsic probes to study the conformation and dynamics of the surface structures to be discussed below.

Surface structure modified by site-directed mutagenesis at the C-terminal α-helices and the vicinity of the E-F loop and a variety of environmental factors

In general, ^{13}C chemical shifts of the backbone C_α and C=O as well as C_β carbons of any given amino-acid residues in proteins and peptides vary by up to 8 ppm, with their local conformations of peptide units defined by a set of two torsion angles (φ and ψ) with reference to those of a series of model polypeptides (Saitô 1986; Saitô and Ando 1989; Saitô et al. 1998, 2002). Accordingly, such specific displacements of peaks have been utilized as excellent intrinsic probes for any given conformational change (Saitô 1986; Saitô and Ando 1989; Saitô et al. 1998, 2000, 2002). Nevertheless, it should be taken into account that these ^{13}C chemical shifts (δ) are time-averaged values between those of various conformers (δ_i), if the exchange rate among them is much faster than the chemical shift difference of the individual conformers defined by a single set of torsion angles as achieved at low temperature:

$$\delta = \Sigma p_i \delta_i \quad (1)$$

where p_i is the fraction of the conformer i under consideration (Yamaguchi et al. 2001a). Particularly, this is the case for the ^{13}C chemical shifts of the loops in bR, because they are far from static but in a time-averaged state between various conformers with correlation times on the order of 10^{-4} s, as manifested from the selectively suppressed ^{13}C NMR peaks of [2-^{13}C]Ala-labeled bR (Yamaguchi et al. 2001a). In such a case, downfield and upfield displacement of peaks from the loops should be interpreted in terms of dynamic conformational changes from a more flexible form to an ordered state and vice versa, respectively, in view of the direction of the displacement toward the peak positions of the highly disordered state at 16.88 ppm.

As pointed out already, such conformational changes could be mediated by formation or disruption of the cytoplasmic surface complex between the C-terminal α-helix, C-D and E-F loops (Yamaguchi et al. 2000, 2001a, 2001b), as judged by the relative displacements of the ^{13}C chemical shifts of [3-^{13}C]Ala-labeled residues in the C-terminal α-helix (Ala228 and Ala233), C-D (Ala103), and E-F (Ala160) loops, as summarized in Tables 1 and 2. In fact, deletion of the C-terminal α-helix by papain or mutation at the C-terminal α-helix and E-F loop resulted in a substantial conformational change in the loop region of the ^{13}C chemical shifts (Ala103 and Ala160) with reference to the data of intact bR (Table 1). Most notably, lowering the temperature of bR from 40 °C to –10 °C resulted in an upfield displacement of the ^{13}C chemical shift of the C-terminal α-helix by about 0.43 ppm (Yamaguchi et al. 2001a). It seems difficult to interpret such temperature-dependent displacement of the ^{13}C chemical shifts of the C-terminal α-helix, as far as an unperturbed (or undistorted) α-helix is taken into account. On the contrary, we previously showed that a fluctuated or perturbed α-helix conformation with a low-frequency motion ($>10^2$ Hz) could be recognized as an α_{II}-helix from ^{13}C NMR data (Kimura et al. 2001), instead of the static picture from IR spectra by Krimm and Dwivedi (1982). In this context, the above-mentioned upfield displacement of the ^{13}C NMR peak of the α-helix form to the normal position, 15.5 ppm at –10 °C, corresponding to the α-helical Ala C_β peak of $(Ala)_n$ in the solid state (Saitô 1986; Saitô and Ando 1989; Saitô et al. 1998, 2002), can be ascribed to a recovery of the perturbed α_{II}-helix to the unperturbed α_I-helix form.

It appears, therefore, that the C-terminal α-helix as an unperturbed form, encountered for WT at low temperature, could be readily visualized as an "open" form

Table 2 Summary of conditions leading to formed or disrupted cytoplasmic complex as judged from the ^{13}C chemical shifts of the C-terminal α-helix

	Formed	Disrupted	Ref
Wild type	Ambient temperature (> 0 °C)	Low temperature (–10 °C)	a
	High ionic strength (> 10 mM NaCl)	Deionized	This work
Mutants	Neutral pH	Low pH (< 4.5)	b
		D85N (pH > 10)	c
		R227Q	This work
		E166G	This work
		A168G	This work

[a]Yamaguchi et al. (2001a)
[b]Tuzi et al. (1999)
[c]Kawase et al. (2000)

consisting of the C-terminal α-helix extended straightforwardly from the G helix. This can be schematically drawn as a cylinder protruding from the membrane surface which is free from mutual interactions with nearby loops, superimposed upon the drawing by Grigorieff et al. (1996) (see Fig. 8A). It is expected that such an "open" form is dominant under conditions such as a pH lower than 4.5 (Yamaguchi et al. 2001a), including deionized or acid blue membranes, or the M-like state of D85N at pH 10 (Kawase et al. 2000) and mutants at the C-terminal α-helix (R227Q) and in the vicinity of the E-F loop (E166G and A168G), because the loop regions and the cytoplasmic ends of the helices acquire motional flexibility with a frequency range up to 10^5 Hz, resulting in the selective suppression of ^{13}C NMR signals (Rothwell and Waugh 1981) of [2-^{13}C] Ala-bR (Yamaguchi et al. 2001b) and 16.38 ppm ascribable to Ala39 (helix B) (Tanio et al. 1999) and Ala168 (helix F), respectively (Fig. 2). In contrast, it is plausible that, in order to facilitate the maximum mutual interactions with the nearby loops, the C-terminal α-helix tilted toward the direction of the B and F helices might be more preferable as a "capped" form (see Fig. 8B). Undoubtedly, this form is more suitable to prevent accelerated fluctuation motions in the cytoplasmic ends of the B and F helices (Fig. 1, gray color) by forming a cytoplasmic structure or a cytoplasmic complex. This means that the cytoplasmic surface complex of the WT at ambient temperature is formed from the C-terminal α-helix and the C-D and E-F loops and probably the A-B loop also, at the expense of the stability of the C-terminal α-helix itself, mainly due to the stereochemical requirement for formation of such a complex through salt bridges from charged residues and/or cation-mediated interactions utilizing divalent cations such as Ca^{2+}.

In many instances, however, such a surface structure should be considered as a rapidly interconverting system, at least between the above-mentioned two forms described in Eq. 1, although the relative proportions of these forms vary depending upon environmental factors such as temperature, pH, ionic strength, etc. It is also pointed out that such a conformational change illustrated in Fig. 8 might be related to the consequence of the conformational switch responsible for proton uptake after release of a proton from the extracellular surface in the photocycle. In this connection, it is mentioned that these findings are obviously consistent with a view that the presence of such a cytoplasmic surface complex plays an important role to facilitate efficient proton uptake by preventing unnecessary fluctuation in the cytoplasmic surface of the WT, by taking into account the recent

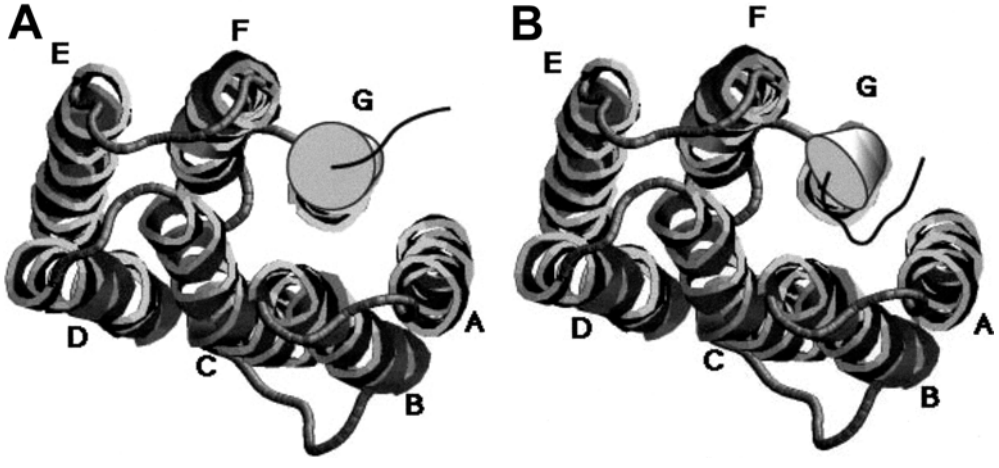

Fig. 8A, B Schematic representation of the relative orientation of the C-terminal α-helix (helix G′ as added *cylinder*) superimposed upon the 3D structure (cytoplasmic side) of bR by Grigorieff et al. (1996). *Small capital letters*, A–G, denote the transmembrane helices. **A** An "open" form in which the C-terminal α-helix is straightforwardly extended from helix G. **B** A "capped" form in which the C-terminal α-helix is tilted toward the direction of the B- and F-helices to be able to interact with the nearby loops through salt bridges and/or metal ion-mediated bonding

findings by Checover et al. (1997, 2001). Brown et al. (1994) also showed that R227 plays an important role through a cluster of interacting residues to facilitate proton transfer from the cytoplasmic domain.

Irreversible conformational change of the surface structure due to Ca^{2+} binding

It is interesting to note that the conformational alterations of the C-D and E-F loops were induced by different concentrations of monovalent and divalent cations. The C-D loop structure was found to be altered by changing the concentration of the monovalent cations, Na^+, from 10 to 50 mM for bR, while the E-F loop was modified by increased Ca^{2+} concentration up to 1 mM. It is notable that such a lower relative concentration of Ca^{2+} of up to 1 mM compared with the concentration of the monovalent cation, 10 mM NaCl, is sufficient to yield a highly altered conformation in the E-F loop, although the effect of the divalent cation turned out to be ineffective in the presence of high monovalent cations up to 100 mM in view of a rapid ligand exchange process (Fig. 3). Nevertheless, there appears no displacement of the ^{13}C chemical shift from the C-terminal α-helix with or without Ca^{2+}.

Further, it is interesting to note that the ^{13}C NMR spectra of Na^+/Ca^{2+}-regenerated bR and A160G prepared by addition of Ca^{2+} to Na^+-regenerated purple membrane without divalent cations are not always the same as those of preparations under ordinary composition of the cations (Figs. 6 and 7). This means that an irreversible surface structure is formed by addition of divalent cations before and after preparation of the purple membrane. This is mainly because binding of monovalent cations to bR seems to modify the electrostatic interaction in a nonspecific manner, while binding of divalent cations seems to favor the most stable topological assembly of the surface as a result of achievement of the octahedral arrangement of surrounding ligands. In such case, the most favored arrangement of the surface complex due to Ca^{2+} binding might not always be the same as the condition to form the most stable C-terminal α-helix, as judged from the specific displacement of ^{13}C NMR peaks. These considerations indicate that there are several sites for cation binding in the cytoplasmic site which are substantially varied, depending upon the conditions of environmental factors such as pH, temperature, etc. In other words, this picture is consistent with a view that no preferred cation-binding sites for divalent cations are available.

Acknowledgements The authors are grateful to Professors Janos K. Lanyi of the University of California, Irvine, USA, and Richard Needleman of Wayne State University, USA, for providing the bR mutants. This work was supported, in part, by a Grant-in-Aid from the Ministry of Education, Culture, Science and Sports of Japan and by the Shorai Foundation for Science and Technology.

References

Ariki M, Lanyi JK (1986) Characterization of metal ion-binding sites in bacteriorhodopsin. J Biol Chem 261:8167–8174

Brown LS, Yamazaki Y, Maeda A, Sun L, Needleman R, Lanyi JK (1994) The proton transfers in the cytoplasmic domain of bacteriorhodopsin are facilitated by a cluster of interacting residues. J Mol Biol 239:401–414

Chang CH, Chen JG, Govindjee R, Ebrey T (1985) Cation binding by bacteriorhodopsin. Proc Natl Acad Sci USA 82:396–400

Checover S, Nachliel E, Dencher NA, Gutman M (1997) Mechanism of proton entry into the cytoplasmic section of the proton-conducting channel of bacteriorhodopsin. Biochemistry 36:13919–13928

Checover S, Marantz Y, Nachliel E, Gutman M, Pfeiffer M, Tittor J, Oesterhelt D, Dencher NA (2001) Dynamics of the proton transfer reaction on the cytoplasmic surface of bacteriorhodopsin. Biochemistry 40:4281–4292

Eliash T, Weiner L, Ottolenghi M, Sheves M (2001) Specific binding site for cations in bacteriorhodopsin. Biophys J 81:1155–1162

Essen L, Siegert R, Lehmann WD, Oesterhelt D (1998) Lipid patches in membrane protein oligomers: crystal structure of the bacteriorhodopsin-lipid complex. Proc Natl Acad Sci USA 95:11673–11678

Grigorieff N, Ceska TA, Downing KH, Baldwin JM, Henderson R (1996) Electron-crystallographic refinement of the structure of bacteriorhodopsin. J Mol Biol 259:393–421

Henderson R, Baldwin JM, Ceska TA, Zemlin F, Beckman E, Downing KH (1990) Model for the structure of bacteriorhodopsin based on high-resolution electron cryo-microscopy. J Mol Biol 213:899–929

Heymann JB, Müller DJ, Landau EM, Rosenbusch JP, Pebay-Peyroula E, Büldt G, Engel A (1999) Charting the surface structure of the purple membrane. J Struct Biol 128:243–249

Jonas R, Ebrey TG (1991) Binding of a single divalent cation directly correlates with the blue-to-purple transition in bacteriorhodopsin. Proc Natl Acad Sci USA 88:149–153

Kawase Y, Tanio M, Kira A, Yamaguchi S, Tuzi S, Naito A, Kataoka M, Lanyi JK, Needleman R, Saitô H (2000) Alteration of conformation and dynamics of bacteriorhodopsin induced by protonation of Asp 85 and deprotonation of Schiff base as studied by ^{13}C NMR. Biochemistry 39:14472–14480

Kimura S, Naito A, Tuzi S, Saitô H (2001) A ^{13}C NMR study on [3-^{13}C]-, [1-^{13}C]Ala-, or [1-^{13}C]Val-labeled transmembrane peptides of bacteriorhodopsin in lipid bilayers: insertion, rigid-body motions, and local conformational fluctuations at ambient temperature. Biopolymers 58:78–88

Kimura Y, Vassylyev DG, Miyazawa A, Kidera A, Matsushima K, Mitsuoka K, Murata K, Hirai T, Fujiyoshi Y (1997) Surface of bacteriorhodopsin revealed by high-resolution electron crystallography. Nature 389:206–211

Krimm S, Dwivedi AM (1982) Infrared spectrum of the purple membrane: clue to proton conduction mechanism? Science 216:407–408

Luecke H, Richter H-T, Lanyi JK (1998) Proton transfer pathways in bacteriorhodopsin at 2.3 Å resolution. Science 280:1934–1937

Luecke H, Schobert B, Richter H-T, Cartailler J-P, Lanyi JK (1999) Structure of bacteriorhodopsin at 1.55 Å resolution. J Mol Biol 291:899–911

Mitsuoka K, Hirai T, Murata K, Miyazawa A, Kidera A, Kimura Y, Fujiyoshi Y (1999).The structure of bacteriorhodopsin at 3.0 Å resolution based on electron crystallography: implication of the charge distribution. J Mol Biol 249:239–243

Müller DJ, Heymann JB, Oesterhelt F, Möller C, Gaub H, Büldt G, Engel A (2000) Atomic force microscopy of native purple membrane. Biochim Biophys Acta 1460:27–38

Oesterhelt D, Stoeckenius W (1974) Isolation of the cell membrane of *Halobacterium halobium* and its fractionation into red and purple membrane. Methods Enzymol 31:667–678

Onishi H, McCance E, Gibbons NE (1965) A synthetic medium for extremely halophilic bacteria. Can J Microbiol 11:365–373

Pardo L, Sepulcre F, Cladera J, Dunach M, Labarta A, Tejada J, Padros E (1998) Experimental and theoretical characterization of the high-affinity cation binding site of the purple membrane. Biophys J 75:777–784

Pebay-Peyroula E, Rummel G, Rosenbusch JP, Landau EM (1997) X-ray structure of bacteriorhodopsin at 2.5 angstroms from microcrystals grown in lipidic cubic phases. Science 277:1676–1681

Riesle J, Oesterhelt D, Dencher NA, Heberle J (1996) D38 is an essential part of the proton translocation pathway in bacteriorhodopsin. Biochemistry 35:6635–6643

Rothwell WP, Waugh JS (1981) Transverse relaxation of dipolar coupled spin systems under rf irradiation: detecting motions in solid. J Chem Phys 75:2721–2732

Saitô H (1986) Conformation-dependent ^{13}C chemical shifts: a new means of conformational characterization as obtained by high-resolution solid-state NMR. Magn Reson Chem 24:835–852

Saitô H, Ando I (1989) High-resolution solid-state NMR studies of synthetic and biological macromolecules. Annu Rep NMR Spectrosc 21:209–290

Saitô H, Tuzi S, Naito A (1998) Empirical vs. nonempirical evaluation of secondary structure of fibrous and membrane proteins. Annu Rep NMR Spectrosc 36:79–121

Saitô H, Tuzi S, Yamaguchi S, Tanio M, Naito A (2000) Conformation and backbone dynamics of bacteriorhodopsin revealed by ^{13}C NMR. Biochim Biophys Acta 1460:39–48

Saitô H, Tuzi S, Tanio M, Naito A (2002) Dynamic aspect of membrane proteins and membrane associated peptides as revealed by ^{13}C NMR: lessons from bacteriorhodopsin as an intact protein. Annu Rep NMR Spectrosc 47:39–108

Sato H, Takeda K, Tani K, Hino T, Okada T, Nakasako M, Kamiya N, Kouyama T (1999) Specific lipid-protein interactions in a novel honeycomb lattice structure of bacteriorhodopsin. Acta Crystallogr Sect D 55:1251–1256

Szundi I, Stoeckenius W (1987) Effect of lipid surface charges on the purple to blue transition of bacteriorhodopsin. Proc Natl Acad Sci USA 84:3681–3684

Szundi I, Stoeckenius W (1989) Surface pH controls purple-to-blue transition of bacteriorhodopsin. Biophys J 56:369–383

Tan EHL, Govender DSK, Birge RR (1996) Large organic cations can replace Mg^{2+} and Ca^{2+} ions in bacteriorhodopsin and maintain proton pumping activity. J Am Chem Soc 118:2752–2753

Tanio M, Inoue S, Yokota K, Seki T, Tuzi S, Needleman R, Lanyi JK, Naito A, Saitô H (1999) Long-distance effects of site-directed mutations on bacteriorhodopsin from solid state NMR of [1-^{13}C]Val-labeled proteins. Biophys J 77:431–442

Tuzi S, Naito A, Saitô H (1994) ^{13}C NMR study on conformation and dynamics of the transmembrane α-helices, loops, and C-terminus of [3-^{13}C]Ala-labeled bacteriorhodopsin. Biochemistry 33:15046–15052

Tuzi S, Yamaguchi S, Tanio M, Konishi H, Inoue S, Naito A, Needleman R, Lany JK, Saitô H (1999) Location of a cation-binding site in the loop between helices F and G of bacteriorhodopsin as studied by ^{13}C NMR. Biophys J 76:1523–1531

Tuzi S, Hasegawa J, Kawaminami R, Naito A, Saitô H (2001) Regio-selective detection of dynamic structure of transmembrane α-helices as revealed from ^{13}C NMR spectra of [3-^{13}C]Ala-labeled bacteriorhodopsin in the presence of Mn^{2+} ion. Biophys J 81:425–434

Váró G, Brown LS, Needleman R, Lanyi JK (1999) Binding of calcium ions to bacteriorhodopsin. Biophys J 76:3219–3226

Wang J, El-Sayed MA (2001) The effect of metal cation binding on the protein, lipid and retinal isomeric ratio in regenerated bacteriorhodopsin of purple membrane. Photochem Photobiol 73:564–571

Yamaguchi S, Tuzi S, Tanio M, Naito A, Lanyi JK, Needleman R, Saitô H (2000) Irreversible conformational change of bacterioopsin induced by binding of retinal during its reconstitution to bacteriorhodopsin, as studied by ^{13}C NMR. J Biochem (Tokyo) 127:861–869

Yamaguchi S, Yonebayashi K, Konishi H, Tuzi S, Naito A, Lanyi JK, Needleman R, Saitô H (2001a) Cytoplasmic surface structure of bacteriorhodopsin consisting of interhelical loops and C-terminal α-helix, modified by a variety of environmental factors as studied by ^{13}C-NMR. Eur J Biochem 268:2218–2228

Yamaguchi S, Tuzi S, Yonebayashi K, Naito A, Needleman R, Lanyi JK, Saitô H (2001b) Surface dynamics of bacteriorhodopsin as revealed by ^{13}C NMR studies on [^{13}C]Aal-labeled proteins: detection of millisecond or microsecond motions in interhelical loops and C-terminal α-helix. J Biochem (Tokyo) 129:373–382

Zhang NY, El-Sayed MA (1993) The C-terminus and the Ca^{2+} low affinity binding sites in bacteriorhodopsin. Biochemistry 32:14173–14175